Published in final edited form as:

Mol Cancer Res. 2024 April 02; 22(4): 360–372. doi:10.1158/1541-7786.MCR-23-0676.

miR-217 regulates normal and tumor cell fate following induction of Endoplasmic Reticulum Stress

Neekkan Dey[1], **Costas Koumenis**[2], **Davide Ruggero**[3], **Serge Y. Fuchs**[4], **J. Alan Diehl**[1,*]

[1]Department of Biochemistry, Case Comprehensive Cancer Center; Case Western Reserve University, Cleveland, OH 44106, USA

[2]Department of Radiation Oncology, Perelman School of Medicine, University of Pennsylvania, Philadelphia, PA 19104, USA

[3]Departments of Urology and Cellular and Molecular Pharmacology, University of California, San Francisco, San Francisco, CA 94158, USA

[4]Dept. of Biomedical Sciences, School of Veterinary Medicine, University of Pennsylvania, Philadelphia, PA 19104, USA

Abstract

Rapidly proliferating cancer cells require a microenvironment where essential metabolic nutrients like glucose, oxygen, and growth factors become scarce as the tumor volume surpasses the established vascular capacity of the tissue. Limits in nutrient availability typically trigger growth arrest and/or apoptosis to prevent cellular expansion. However, tumor cells frequently co-opt cellular survival pathways thereby favoring cell survival under this environmental stress. The Unfolded Protein Response (UPR) pathway is typically engaged by tumor cells to favor adaptation to stress. PERK, an endoplasmic reticulum (ER) protein kinase and UPR effector is activated in tumor cells and contributes tumor cell adaptation by limiting protein translation and balancing redox stress. PERK also induces micro-RNAs that contribute to tumor adaptation. miR-211 and miR-216b were previously identified as a PERK-ATF4 regulated micro-RNAs that regulate cell survival. We have identified another PERK responsive miRNA, miR-217, with increased expression under prolonged ER stress. Key targets of miR-217 are identified as *TRPM1*, the host gene for miR-211 and *EZH2*. Evidence is provided that miR-217 expression is essential for the rapid loss of miR-211 in prolonged ER stress and provides a functional link for determining whether cells adapt to stress or commit to apoptosis.

Keywords

UPR; PERK; miR-217; apoptosis

*Correspondence jad283@case.edu.

D.R. is a shareholder of eFFECTOR Therapeutics, Inc., and a member of its scientific advisory board. Other authors declare no competing interests.

Introduction

The ER is the site of secretory protein maturation and folding and is thus a sensor of stress that impact proteostasis. Limitations in glucose and oxygen availability or alterations in redox status, which commonly occur during tumorigenesis, rapidly triggers protein misfolding in the ER and activates a signal transduction pathway referred to as the UPR. The critical function of the ER in sensing alterations in key nutrients, makes the ER and the UPR pathway key for tumor cell adaptation to nutrient and proteotoxic stress.

Activation of the UPR signals a reduced rate of protein translation to diminish ER protein traffic while simultaneously inducing expression and translation of ER chaperones and a pro-survival transcription factor, ATF4. UPR activation also inhibits cell cycle progression [1] and modulates cell survival or cell death responses in both normal and tumor-derived cells [2–5]. Mammalian cells contain three ER transmembrane protein kinases (PERK, Ire1α, and ATF6) that function as effectors of the UPR. PERK is the central regulator of cell homeostasis and cell survival. PERK regulates cell survival through increased translation and function of the ATF4 transcription factor and through inhibition of cell division by repressing translation of G1 cyclins [1, 6, 7].

Studies from multiple research teams have shown that each of the three branches of the UPR regulates distinct subsets of micro-RNAs. The modes of regulation include Ire1-mediated micro-RNA degradation[8, 9] or processing [10, 11] as well as ATF4- and ATF6-dependent transcription targets [12–16]. PERK signaling through ATF4 has been linked to pro-apoptotic miR-216b and anti-apoptotic miR-211 [17]. The ability of PERK-dependent miRNAs to regulate cell death suggests their potential to directly regulate cell fate of cells exposed to physiological stress.

In the current work, we describe the identification of a key micro-RNA, miR-217, that supports a role for PERK regulated miRNAs in cell fate decisions. MiR-217 expression is differentially regulated in numerous cancers including pancreatic cancer [18, 19], thyroid cancer [20], gastric cancer [21], lung cancer[22], clear cell renal cell carcinoma [23], osteosarcoma [24], ovarian cancer [25], triple negative breast cancer [26], hepatocellular carcinoma [27], glioblastoma [28], and colorectal cancer [29]. Depending on the study and cancer type, miR-217 has potential pro-tumorigenic and anti-tumorigenic functions. In the work discussed below, we characterize UPR-dependent regulation of miR-217 and its role in the regulation of cell fate following ER stress.

Materials and Methods

Cell culture.

NIH3T3 fibroblasts (American Type Culture Collection (ATCC, RRID:CVCL_0594), murine embryonic fibroblasts (MEFs) and 293T human embryonic kidney cells (ATCC, RRID:CVCL_0045) were maintained in DMEM (10-013-CM, Corning®) with 10% heat-inactivated fetal bovine serum and 1% penicillin–streptomycin. MEFs were supplemented with 10% fetal calf serum, 2 mM L-glutamine (Cat# 25030081, Gibco™), 55 mM β-mercaptoethanol (Cat# 1610710, Bio-Rad) and MEM nonessential amino acid mix

(containing alanine, aspartate, asparagine, glutamate, glycine, proline and serine), all from Invitrogen. U2OS human cervical adenocarcinoma cells (HTB-96™, ATCC, RRID:CVCL_0042) were maintained in McCoy's 5A with 10% heat-inactivated fetal bovine serum, pen/strep. Human AGS (CRL-1739, ATCC, RRID:CVCL_0139) gastric adenocarcinoma cells were maintained in ATCC-formulated F-12K Medium (Cat# 30-2004) with 10% heat-inactivated fetal bovine serum and 1% penicillin–streptomycin. Cell purchased directly from ATCC as indicated and authenticated by ATCC. Cells were periodically confirmed to be free of mycoplasma contamination using the Universal Mycoplasma Detection Kit (30-1012K, ATCC).

Plasmids and chemicals.

Scrambled miR-control (Cat# CmiR0001-MR03), miR-217 (Cat# MmiR3269-MR03), A-miR-217 (Cat# MmiR-AN0933-AM03), 3'UTR-Vector Control (Cat# CmiT000001-MT06), Wt-EZH2-3'UTR (Cat# MmiT073625-MT06), Wt-SUZ12-3'UTR (Cat# HmiT088547-MT06) and EZH2 expression plasmid (Cat# EX-Z0388-Lv242) vectors were purchased from GeneCopoeia. PERK inhibitor was purchased from Selleckchem (Cat# GSK-2606414). Thapsigargin (Cat# T9033, Sigma-Aldrich), IRE1 Inhibitor III 4μ8C (Cat# 412512, Sigma-Aldrich), EZH2 inhibitor Tazemetostat (EPZ-6438) (Cat# S7128, Selleck Chemicals), Actinomycin D (A9415, Sigma-Aldrich), Puromycin (P7255, Sigma-Aldrich), Hygromycin B (Cat# 10687010, Gibco™), APC Annexin V (BD 550474), Propidium iodide (Cat# P4170, Sigma-Aldrich), RNase (Cat# 10109134001, Roche), High-Capacity cDNA Reverse Transcription Kit with RNase Inhibitor (Cat# 4374966, Applied Biosystems™), TURBO DNA-free™ Kit (Cat# AM1907, Invitrogen™).

MicroRNA purification and qPCR.

NIH 3T3 or AGS cells were challenged with Tg (300 nM) for 2, 5 or 10 h. Total miRNA was purified after appropriate treatments using mirVana™ miRNA Isolation Kit (Invitrogen™, Cat.# AM1560) or miRNeasy Mini Kit (Cat.# 217084, Qiagen) as per the manufacturer's instructions. MicroRNA was reverse transcribed using TaqMan™ MicroRNA Reverse Transcription Kit (Cat.# 4366596, Applied Biosystems™) with specific Taqman RT primers (TaqMan® Gene Expression Assays) for mmu-miR-217* (Cat.# 4440886, Assay ID 464097_mat), hsa-miR-217 (Cat.# 4427975, Assay ID 002337), mmu-miR-211 (Cat.# 4427975, Assay ID 001199), mmu-miR-211* (Cat.# 4440886, Assay ID 463128_mat), hsa-miR-211 (Cat.# 4427975, Assay ID 000514), Taqman™ Pri-miRNA Assay (hsa-mir-211) (Cat.# 4427012, Assay ID Hs03302954_pri), TaqMan™ Non-coding RNA Assay MIR211 (Human, pre-miRNA, Cat.# 4426961, Assay ID Hs04231471_s1), TaqMan™ Non-coding RNA Assay MIR211 (Mouse, pre-miRNA, Cat.# 4426961, Assay ID Mm04238237_s1), Trpm1 (Mouse, Cat.# 4331182, Assay ID Mm00450619_m1), Trpm1 (Human, Cat.# 4331182, Assay ID Hs00931865_m1), Chop (Ddit3) (Mouse, Cat.# 4331182, Assay ID Mm01135937_g1), GAPDH (Human, Cat.# 4331182, Assay ID Hs02786624_g1), Gapdh (Mouse, Cat.# 4331182, Assay ID Mm99999915_g1), USB1 (Human, Cat.# 4331182, Assay ID Hs00984809_m1) and miR-202 (Cat. # 4427975, Applied Biosystems) as per the manufacturer's protocol. qPCR was performed on an Applied Biosystems 7900 qRT-PCR machine (Applied Biosystems™). qPCR was performed with specific Taqman PCR primers

using TaqMan™ Universal PCR Master Mix (Cat. # 4304437, Applied Biosystems™). Relative fold changes were calculated using the $\Delta\Delta C_t$ method.

Retroviruses and stable AGS/NIH 3T3 cells.

293T cells were transfected with PMDL, VSVG, REV and vector containing miR-217 mimic (Cat# MmiR3269-MR03, Gene-Copoeia) or A-miR-217 (Cat# MmiR-AN0933-AM03) or scrambled miR-Control (Cat# CmiR0001-MR03, GeneCopoeia) using Lipofectamine (Cat# 18324012, Invitrogen™) and PLUS™ Reagent (Cat# 11514015, Invitrogen™). Viral supernatants were harvested 48 h after transfection and were used to infect AGS and NIH3T3 cells in the presence of 10 μg/ml polybrene (TR-1003, Sigma-Aldrich). Selection to create stably miR-217 overexpressing cells was conducted with puromycin (P7255, Sigma-Aldrich) at 2 mg/ml, or for anti-miR-217 with 0.2 mg/ml Hygromycin B (Cat# 10687010, Invitrogen™) [6].

Luciferase assays.

For miR-217-EZH2 luciferase assays, mut-EZH2-3'UTR construct was generated by QuikChange II XL Site-Directed Mutagenesis Kit (Cat# 200521, Agilent Technologies) using primers: forward 5'-cagtactttgcaaattcagaatttcaaaacggctttccgttttctaaattgcccacagtact-3' and reverse 5'-agtactgtgggcaatttagaaaacggaaagccgttttgaaattctgaatttgcaaagtactg-3'). 3'UTR-Vector Control (Cat# CmiT000001-MT06, GeneCopoeia) or Wt-EZH2-3'UTR (Cat# MmiT073625-MT06, GeneCopoeia, Supplementary Figure. 3b) or Mut-EZH2-3'UTR (generated by SDM) reporter construct was independently expressed in scrambled miR-Control (Cat# CmiR0001-MR03, GeneCopoeia), miR-217 (Cat# MmiR3269-MR03, GeneCopoeia) and A-miR-217 (Cat# MmiR-AN0933-AM03, GeneCopoeia) expressing NIH3T3 cells, respectively and treated with Tg (300 nM) for the time wherever indicated. For miR-217-SUZ12 luciferase assays, 3'UTR-Vector Control (Cat# CmiT000001-MT06, GeneCopoeia) or Wt-SUZ12-3'UTR (Cat# HmiT088547-MT06, GeneCopoeia, Supplementary Figure. 4b) or Mut-SUZ12-3'UTR (generated by SDM using primers: forward 5'-taatgacatcaataaaagtgatatacatgtaatgacggctaatgaagtgaagtagaaccctgatacaaatatc-3' and reverse 5'-gatatttgtatcagggttctacttcacttcattagccgtcattacatgtatatcacttttattgatgtcatta-3') reporter construct was independently expressed in scrambled miR-Control (Cat# CmiR0001-MR03, GeneCopoeia), miR-217 (Cat# MmiR3269-MR03, GeneCopoeia) and A-miR-217 (Cat# MmiR-AN0933-AM03, GeneCopoeia) expressing NIH3T3 cells, respectively and treated with Tg (300 nM) for the time wherever indicated. Firefly luciferase (hLuc) activity was measured and normalized to transfection control Synthetic Renilla Luciferase using Luc-Pair™ Duo-Luciferase HS Assay Kit, (Cat# LF004, GeneCopoeia).

Western blot analysis.

Cells were harvested by gently scraping and resuspended in EBC buffer (50 mM Tris-HCl, pH 7.5, 100 mM NaCl, 0.5% Nonidet P-40) supplemented with protease inhibitors. The cells were disrupted by sonication and then cleared by microcentrifugation at 10,000g for 10 min. Protein lysates were quantified using Protein Assay Dye Reagent Concentrate (Bio-Rad, #5000006). 40 μg of each protein sample was loaded, resolved by SDS–polyacrylamide gel electrophoresis, transferred onto nitrocellulose membrane and analyzed by immunoblot. Antibodies used were as follows: PERK (C33E10) rabbit monoclonal antibody (#3192,

Cell Signaling Technology, RRID:AB_2095847), eIF2α Antibody (#9722, Cell Signaling Technology, RRID:AB_2230924), p-eIF2α (Ser51) (119A11) rabbit monoclonal antibody (#3597, Cell Signaling Technology, RRID:AB_390740), ATF4 (D4B8) rabbit monoclonal antibody (#11815, Cell Signaling Technology, RRID:AB_2616025), CHOP mouse monoclonal antibody (#2895, Cell Signaling Technology, RRID:AB_2089254), cleaved caspase 3 (#9661, Cell Signaling Technology, RRID:AB_2341188), Ezh2 (D2C9) XP® rabbit monoclonal antibody (#5246, Cell Signaling Technology, RRID:AB_10694683), SUZ12 (D39F6) XP® rabbit monoclonal antibody (#3737, Cell Signaling Technology, RRID:AB_2196850), Tri-Methyl-Histone H3 (Lys27) (C36B11) rabbit monoclonal antibody (#9733, Cell Signaling Technology, RRID:AB_2616029), TRPM1 Polyclonal Antibody (Cat #OSR00049W, Thermo Fisher Scientific, RRID:AB_962349) and actin (Sigma). Antibody binding was visualized by enhanced chemiluminescence (Perkin Elmer). The same blot was used to check the level of different proteins based on their molecular weights and if required, the blots were stripped and reprobed.

Flow cytometric analysis.

Apoptosis was quantified using the APC annexin V (Cat# 550474, BD Biosciences, RRID:AB_2868885). FACS (fluorescence-activated cell sorting) was performed on a BD Accuri C6 Plus (BD Biosciences, RRID:SCR_014422) and analyzed by FlowJo (TreeStar, RRID:SCR_008520). The procedure was performed according to the manufacturer's instructions. Briefly, after indicated treatment single cell suspensions were prepared, washed with cold PBS, and then resuspended in 1× binding buffer (BD 556454, RRID:AB_2869074) at a concentration of 1×10^6 cells ml^{-1}. Subsequently, 100 μl of the solution was transferred to a tube, and 5 μl APC annexin V was added. After gentle vortexing, the cells were incubated for 15 min at room temperature in dark. Finally, a volume of 400 μl volume of 1× binding buffer was added to each tube, and flow cytometric analysis was conducted within 1 h.

Clonogenic survival assay.

Clonogenic assays were performed in AGS stable cells as previously described [30, 31]. Briefly, cells were plated at $2x10^3$ cells per 60 mm plates. Twenty-four hours later, they were exposed to Tg (300 nM) for the indicated times, then returned to growth medium. Fresh culture media were replenished every 2 days. Finally, viable colonies were stained with 3 ml of 0.5% Giemsa (v/v) for 5-10 min at room temperature on the 12^{th} day. Colony counts were normalized to plating efficiency and represented as fraction surviving compared to control. Colonies were quantified in a blinded fashion.

Data Availability.

The data generated in this study are available within the article and its supplementary data files.

Sex as a biological variable.

Not considered in the current study given use of standard cell lines.

Statistical Analysis.

Data were collected and handled in either GraphPad 8 (RRID:SCR_002798) or Microsoft Excel. Statistical analysis for all assays provided in figure legends.

Results

miR-217 is induced by the UPR.

Previous experiments focused on the identification of micro-RNAs regulated by the UPR revealed a significant increase in the expression of several miRNAs including those in the miR-200 cluster [17, 31]. Because miR-217 is differentially regulated in multiple cancers, we focused on miR-217. To validate stress-dependent accumulation of miR-217, RNA was collected from thapsigargin-challenged NIH3T3 cells over a time course of 24hrs. MiR-217 expression induction was evident at 5 hrs and accumulation was noted over the 24h interval (Fig 1a). We next compared expression of miR-217 with that of validated stress responsive mRNA, *chop* in response to an independent inducer of the UPR, tunicamycin. While *chop* expression was evident by 2h, miR-217 induction was again noted by 5 hours with a significant increase at 10h (Fig 1b). Increased expression of miR-217 was also observed in response to low glucose (Fig. 1c).

miR-217 induction is PERK, ATF4 and CHOP-dependent.

To investigate the regulation of miR-217 expression by UPR signal transducers, we initially focused on PERK, an established regulator of the miR-200 cluster following ER stress [17, 31]. Murine embryonic fibroblasts (MEFs) with either intact (PERK+/+) or deficient (PERK−/−) PERK were treated with Tg (300nM), and miR-217 expression was evaluated using quantitative PCR (qPCR). PERK deficiency was confirmed by western blot , as well as through assessment of CHOP accumulation following ER stress (Fig. 2a). MiR-217 was observed to accumulate in PERK+/+ cells but not in −/− cells (Fig. 2a, right). To further validate the reliance of miR-217 expression on PERK activity, we employed GSK2606414 (GSK414), a highly specific small-molecule inhibitor of PERK [32]. GSK414 effectively suppressed PERK activation and miR-217 induction (Fig. S1a), while the IRE1 inhibitor had no impact.

Previous studies indicated that PERK-dependent regulation of gene expression is often reliant on increased accumulation of the ATF4 transcription factor, a process contingent on PERK-mediated eIF2α phosphorylation [5, 33, 34]. MiR-217 induction was abolished in ATF4−/− MEFs in comparison to ATF4 +/+ MEFs (Fig. 2b), as well as in mutated eIF2α A/A MEFs compared to wild-type eIF2α S/S MEFs (Fig. S1b).

As reported previously, ATF4 accumulation occurs within the first 2hrs of ER stress [35] and miR-217 accumulation initially occurs at 5 h, we considered the possibility that ATF4-dependent regulation was indirect. Therefore, we focused our attention on CHOP, a direct transcriptional target of ATF4 [36]. Consistent with a role for CHOP, MiR-217 induction was abolished in CHOP−/− MEFs (Fig.2c). These data demonstrate that ER stress-dependent induction of miR-217 reflects a pathway minimally composed of PERK, ATF4, and CHOP.

ATF4 and CHOP share a set of target genes with the preference of binding to the similar motifs (GCATCAT/G) [4, 37, 38]. Studies indicate that miRNAs that are within adjacent regions and transcribed in the same orientation can form miRNA clusters. Most clusters contain two to three miRNAs, and different miRNAs within a cluster can have different targets. miR-217 is located at the human chromosome 2p16.1, sharing the miR-216a-216b-217 cluster. miRbase indicates that miR-217 is in the same miRNA cluster to that of miR-216a; therefore, miR-217 will share the same promoter as miR-216b (Fig. S1d). Previous work demonstrated miR-216b/217 is a direct target of CHOP by chromatin IP [17]. Under the same conditions, there was no apparent enrichment of ATF4 on the miR-216b/217 promoter, although binding of ATF4 to the CHOP promoter was confirmed. Therefore, miR-217 is apparent to be a direct CHOP transcriptional target.

Actinomycin D before Tg treatment suppressed miR-217 expression, consistent with transcription dependence (Fig. 2d). Finally, miR-217 expression was significantly reduced in Dicer$^{-/-}$ cells compared to control cells, consistent with Dicer dependence (Fig. 2e) [17].

Regulatory tension of miR-211 and miR-217 under ER-stress

PERK induces pro-survival miRNA miR-211, and miR-211 in turn suppresses *chop* gene expression by promoting EZH2-dependent promoter methylation [31]. Because miR-211 expression is transient, miR-211 delays chop expression and CHOP pro-apoptotic signaling [31]. Consequently, miR-211 induction permits cell adaptation to transient acute stress, but under conditions of chronic stress, the transient nature of miR-211 function will be bypassed and cells commit to apoptosis. The mechanism that mediates miR-211 downregulation after 5 hours to ensure its transient accumulation represents a gap in knowledge. Significantly, increased miR-217 expression coincides miR-211 downregulation (Fig 3b). TargetScan (RRID:SCR_010845) analysis revealed putative miR-217 seed sequences in the 3'UTR of the Trpm1 mRNA (Fig 3a). To investigate potential regulatory tension between miR-211 and miR-217, AGS cells expressing control, a miR-217 mimic or Anti-miR-217 were treated with Tg (Fig 3b). Expression of the miR-217 mimic suppressed miR-211; in contrast, in cells expressing an anti-miR-217, basal expression of miR-211 was significantly elevated and miR-211 expression was further elevated throughout 16h of ER stress and not subjected to downregulation (Fig 4a).

Because miR-211 is excised from a trpm1 intron thereby making miR-211 expression dependent on expression of *trpm1* [31], we reasoned that *trpm1* mRNA should be regulated by miR-217. Consistently, the miR-217 mimic suppressed *trpm1* expression following ER stress (Fig 4b) while anti-miR-217 elevated basal *trpm1* and provided sustained *trpm1* expression throughout ER stress (Fig 4b). In addition, it was noted that miR-217 expression also suppressed both pri-miR-211 and pre-miR-211, while anti-miR-217 elevated both (Fig 4c–d).

Finally, we considered whether loss of miR-211 between 5-10h of ER stress reflected altered miR-211 stability or reduced expression as a consequence of miR-217 accumulation. To address this question, we measured miR-211 loss by exposing cells to Tg and at 5hr introducing actinomycin D to prevent new transcription. We reasoned that if miR-211 loss reflected miR-217 regulation of *trpm1* expression, then suppression of miR-217 with

actinomycin D would facilitate continued accumulation of miR-211. Exposure of cells to ER stress promoted miR-211 accumulation by 5h and loss by 10h. In contrast, addition of actinomycin D at 5h, resulted in continued accumulation of miR-211 (Fig S2a). This continued accumulation reflects processing of miR-211 from transcripts that accumulated prior to actinomycin D and suggests that ongoing miR-217 mediated loss of the trpm1 transcript mediated miR-211 loss from 5h onward. As expected, expression of miR217 was suppressed between 5-10h in the presence of actinomycin D (Fig. S2a). Consistent with miR-217 mediating miR-211 suppression, overexpression of the miR-217 mimic triggered a time-dependent loss of miR-211 in the absence or presence of actinomycin D independent of ER stress (Fig S2b). The accelerated loss of miR-211 at 5-10h reflects elevated endogenous miR-217 at later time points (Fig. S2b). Collectively, these data suggest miR-217 antagonizes miR-211 accumulation and induction through targeting of *trpm1* (Fig 4e).

EZH2 is a target of miR-217 following induction of ER stress

To identify miR-217 targets, we searched the 3'UTR region of annotated cDNAs for the presence of matches to the miR-217 seed sequence using a computational algorithm TargetScan. We also examined promoter-proximal regions for potential miR-217 matches, given accumulating evidence for the involvement of miRNAs in transcriptional repression [31, 39]. While many potential targets were identified, the relevance of most putative targets to ER stress signaling was not immediately apparent, as they were not differentially regulated by ER stress. However, EZH2 was noted to be a high relevance target (Fig. 5a; Fig S3a), containing two potential miR-217 sites in its 3'UTR. Given previous data linking EZH2 to the regulation of chop and bmal1 [30], we considered it a potentially relevant target of miR-217.

EZH2 levels decrease between 5-10h of ER stress (Fig. 5b). To assess the contribution of miR-217 to stress-dependent inhibition of EZH2, AGS cells that stably overexpressing a miR-217 mimic or an anti-miR-217 were generated and exposed to a time-course of Tg treatment. Cells expressing miR-217 mimic exhibited reduced basal EZH2 levels and increased kinetics of EZH2 loss relative to control (Fig. 5b). Conversely, expression of A-miR-217 rescued the expression of EZH2 and a significantly maintained the level of EZH2 during ER stress (Fig. 5b).

A luciferase reporter (Fig. S3b) was generated harboring either the wild-type EZH2 3′UTR or one with mutated miR-217 seed sequences (Fig. 5a). Expression of the Luciferase-EZH2 reporter was suppressed by miR-217 mimic in a seed-dependent manner (Fig. 5c). Additionally, wild-type, but not the mutant Luciferase-EZH2 reporter, was responsive to ER stress, while A-miR-217 reduced UPR-dependent regulation (Fig. 5c). Transfection of the miR-217 mimic reduced luciferase expression to 55% of control with inclusion of the Wt-EZH2-3'UTR (Fig 5c). The miR-217 mimic did not impact luciferase expression in the absence of the EZH2 3'UTR (Fig 5c; MT06-vector control). Likewise, miR-217 failed to regulate luciferase expression when miR-217 seed sequences in the EZH2 3'UTR were mutated (Fig 5c). We confirmed that Tg exposure for 5h and 10h reduced luciferase activity levels to 27% and 69% respectively (Fig 5d). As predicted, Tg exposure did not impact

expression of the EZH2 3'UTR reporter when cells were co-transfected with A-miR-217 or Mut-EZH2-3'UTR (Fig. 5d). Co-expression analysis (ENCORI,[40]) reveals negative correlation between miR-217 and EZH2 in different human cancers (Fig. S1c).

miR-217 regulates SUZ12

We noted that SUZ12, another PRC2 component, contains high relevance matches for the miR-217 seed sequence in its 3'UTR (Fig. S4a). To test the relationship between miR-217 and SUZ12, we generated a luciferase reporter harboring either the wild-type 3′UTR of SUZ12 or one with mutated seed sequence (Fig. 6a; Fig. S4b). Expression of the Luciferase-SUZ12 reporter was suppressed by miR-217 mimic in a seed-dependent manner (Fig. 6b). Additionally, wild-type, but not the mutant Luciferase-SUZ12 reporter, was responsive to ER stress, while A-miR-217 abrogated UPR-dependence. Co-transfection of miR-217 (MmiR3269-MR03) and Wt-SUZ12-3'UTR (HmiT088547-MT06) reduced luciferase activity levels to about 36% in NIH3T3 cells compared to the controls, whereas co-transfection of miR-217 and Mut-SUZ12-3'UTR or A-miR-217 and Wt-SUZ12-3'UTR or A-miR-217 and Mut-SUZ12-3'UTR did not reduce these levels significantly (Fig. 6b).

To address ER stress responsiveness, expressing Wt-SUZ12-3'UTR-luciferase were treated with Tg for 5-10hrs; luciferase activity levels were suppressed to 23% and 47% respectively (Fig 6c). However, Tg exposure for 5 or 10hrs to NIH3T3 cells co-transfected with A-miR-217 and Wt-SUZ12-3'UTR or A-miR-217 and Mut-SUZ12-3'UTR did not reduce these levels significantly (Fig. 6c). Tg treatment for 16hrs to $CHOP^{+/+}$ MEFs significantly reduced SUZ12 protein levels compared to $CHOP^{-/-}$ MEFs (Fig. 6d). We surmised that if ER stress can suppress both EZH2 and SUZ12, it stands to reason that UPR activation should suppress methylation of histone H3 at lysine 27. Indeed, we noted a time-dependent decrease in H3K27me3 (Fig. 6d). Consistent with miR-217 expression being CHOP-dependent, UPR-dependent suppression of H3K27me3 was suppressed in CHOP knockout cells (Fig 6d). The suppression of H3K27me3 coincided with no miR217 induction in $CHOP^{-/-}$ cells (Fig 6e).

miR-217 induced suppression of miR-211 Regulates ER Stress-Dependent Apoptosis

Consistent with the role of miR-217 as a regulator of cell survival, we observed overexpression of miR-217 increased Tg-induced apoptosis (Fig. 7a–b). Conversely, cells expressing A-miR-217 exhibited significant resistance to apoptosis (Fig. 7a–b). To independently assess cell survival, we exposed AGS cells expressing Control, miR-217 and A-miR-217 to Tg for 0, 1 or 2 h before supplying fresh Tg-free medium for cell recovery over 12 days. Surviving cells/colonies were quantified, revealing that miR-217-expressing AGS cells were significantly more sensetive to stress compared to Control, while A-miR-217-expressing cells were resistant to Tg-induced death (Fig. 7c). Cell doubling times remained unaffected by either A-miR-217 expression or overexpression of miR-217 mimic, confirming that miR-217 regulates cell viability rather than proliferation (Fig. 7d). Moreover, to confirm the role of EZH2 in ER stress-induced cell death, both Control and EZH2-expressing AGS cells were exposed to Tg for 0, 1, or 2 hours in the presence or absence of the EZH2 inhibitor (Tazemetostat). Afterward, cells were supplied with Tg-free fresh medium and allowed to recover for 12 days. The quantification of surviving colonies

showed that inhibition of EZH2 heightened sensitivity to stress, while EZH2 expression conferred resistance to Tg-induced death (Fig. 7e).

DISCUSSION

Micro-RNAs regulated by the UPR play a significant role in the regulation of cell fate following ER stress. Although all the three main transducers of the UPR, PERK, Ire1, and ATF6, have been associated with miRNA regulation, recent studies indicate that much of the miRNA regulation that influences cell fate occurs through the PERK arm of the UPR. PERK induces pro-survival miRNA miR-211 in an ATF4-dependent manner [31]. MiR-211 in turn directly targets the proximal chop/gadd153 promoter, increases H3K27 trimethylation, and delays chop accumulation. Because miR-211 accumulation is transient, reaching maximum levels by 5 hours of stress and reduced to basal levels by 8-10 hours, miR-211 induction provides a window of opportunity for the cell to reestablish homeostasis prior to apoptotic commitment; its rapid loss coincides with increased cell death. The mechanism of miR-211 downregulation represents a gap in knowledge regarding cell commitment to stress resolution versus cell death.

We have identified another PERK responsive miRNA, miR-217, with increased expression under prolonged ER stress as miR-211 is suppressed. ER stress-dependent induction of miR-217 reflects a pathway minimally composed of PERK, eIF2α, ATF4, and CHOP. Our work demonstrates that miR-217 directly targets two of the major components of PRC2 complex- the Ezh2 methyltransferase, as well as SUZ12 thereby increasing premature CHOP accumulation, ultimately sensitizing cells to ER stress-dependent apoptosis under prolonged ER-stress. Understanding the consequences of PRC2 suppression under prolonged ER stress is essential for unraveling the molecular mechanisms underlying ER stress response and its impact on cell fate [30, 31]. Destabilization of Polycomb repressive complex 2 (PRC2) has significant implications for cellular processes and gene regulation. The potential consequences of PRC2 loss includes reduced gene silencing, altered cell differentiation, dysregulated cell proliferation, impaired DNA repair, and altered chromatin structure. The role of PRC2 in gene silencing through the deposition of repressive histone marks (H3K27me3) is crucial for maintaining proper gene expression and developmental programs. Suppression of PRC2 can disrupt this process, leading to aberrant gene expression and contributing to the development or progression of diseases. PRC2 complex is also involved in cell fate determination and differentiation, which makes it critical for proper cell differentiation during development, and its loss can interfere with this process, potentially resulting in developmental defects. Dysregulation of cell proliferation, another consequence of PRC2 destabilization, can disrupt the balance of cell cycle progression and growth-regulating genes. It is worth noting that the specific effects of PRC2 suppression may vary depending on the cellular context, specific target genes, and cell type. Further research is necessary to gain a comprehensive understanding of the functional outcomes associated with miR-217 mediated PRC2 destabilization in diverse biological systems.

Cancer exhibits both increased and decreased activity of the Polycomb Repressive Complex 2 (PRC2), and the mechanisms underlying these alterations are not fully elucidated. PRC2 consists of core subunits, namely Extraembryonic Ectoderm Development (EED),

Suppressor of Zeste 12 (SUZ12), and the methyltransferase Enhancer of Zeste 2 (EZH2) [41]. Elevated-levels of EZH2 occur in several malignancies [42], and activated mutants of EZH2 are present in diffuse large B cell lymphoma and follicular lymphoma [43, 44]. In contrast, EZH2 is somatically inactivated in myelodysplastic syndrome, myeloproliferative neoplasm, and CALM-AF10 leukemia [45–48]. PRC2 components are also deactivated in T-lineage acute lymphoblastic leukemia [49] and early T-cell precursor (ETP)-acute lymphoblastic leukemia [50].

Induction of miR-217 occurs five hours into the stress response, suggesting its involvement in the decision between cell survival and death. Experimental evidence supports this conclusion, as miR-217 expression depends on the activity of another pro-apoptotic factor called CHOP. Reducing miR-217 levels increases cell resistance to UPR-induced cell death, while its overexpression promotes apoptosis. MiR-217 also has the capacity to target the 3'UTR of Trpm1 gene that harbors miR-211 in its intronic sequence. The kinetics of miR-217 induced regulation of Trpm1 expression is analogous to that of pri-211, pre-211 and mature miR-211. This work suggests a model for the mechanism of decreased miR-211 expression following prolonged ER stress.

While miR-211 induction is transient in response to stress in cultured cells, we previously demonstrated that it accumulates in cancers such as B-cell lymphoma [30]. Thus, some aspect of feedback regulation on miR-211 is lost in some cancers. We considered whether this reflects loss of miR-217 in certain cancers. Co-expression analysis of miR-217 and EZH2 in different human cancers using ENCORI indicated that a strong negative correlation (Fig. S1c), which implies that miR-217 likely plays a role in negatively regulating the expression of EZH2 in the context of various human cancers. The specific implications of this negative correlation would however depend on the functions of miR-217 and EZH2 in the particular types of cancers under investigation.

In summary, our study proposes a model (Fig. S7) where miR-211, induced by PERK during ER stress, promotes cell survival by attenuating *chop* expression early in the ER stress response, but miR-217 mediated silencing of miR-211 permits maximal CHOP accumulation and thereby apoptosis during prolonged stress. Thus, while PERK promotes cell survival via miR-211, it also sets the stage for cellular demise by controlling the onset of miR-217 expression. Collectively, our data provides direct insight into the molecular mechanisms by which PERK induced miRNAs coordinate cell fate in response to proteotoxic activation of the UPR.

Supplementary Material

Refer to Web version on PubMed Central for supplementary material.

ACKNOWLEDGEMENTS

This work was supported by National Institutes of Health grants P01CA165997 (CK, DR, SYF, JAD).

References

1. Brewer JW, et al. Mammalian unfolded protein response inhibits cyclin D1 translation and cell-cycle progression. Proc Natl Acad Sci U S A, 1999. 96(15): p. 8505–10. [PubMed: 10411905]
2. Zhang P, et al. The PERK eukaryotic initiation factor 2 alpha kinase is required for the development of the skeletal system, postnatal growth, and the function and viability of the pancreas. Mol Cell Biol, 2002. 22(11): p. 3864–74. [PubMed: 11997520]
3. Lee AS and Hendershot LM, ER stress and cancer. Cancer Biol Ther, 2006. 5(7): p. 721–2. [PubMed: 16880733]
4. Ma Y and Hendershot LM, The role of the unfolded protein response in tumour development: friend or foe? Nat Rev Cancer, 2004. 4(12): p. 966–77. [PubMed: 15573118]
5. Harding HP, et al. Perk is essential for translational regulation and cell survival during the unfolded protein response. Mol Cell, 2000. 5(5): p. 897–904. [PubMed: 10882126]
6. Brewer JW and Diehl JA, PERK mediates cell-cycle exit during the mammalian unfolded protein response. Proc Natl Acad Sci U S A, 2000. 97(23): p. 12625–30. [PubMed: 11035797]
7. Hamanaka RB, et al. PERK and GCN2 contribute to eIF2alpha phosphorylation and cell cycle arrest after activation of the unfolded protein response pathway. Mol Biol Cell, 2005. 16(12): p. 5493–501. [PubMed: 16176978]
8. Byrd AE and Brewer JW, Micro(RNA)managing endoplasmic reticulum stress. IUBMB Life, 2013. 65(5): p. 373–81. [PubMed: 23554021]
9. Hollien J, et al. Regulated Ire1-dependent decay of messenger RNAs in mammalian cells. J Cell Biol, 2009. 186(3): p. 323–31. [PubMed: 19651891]
10. Lerner AG, et al. IRE1alpha Induces Thioredoxin-Interacting Protein to Activate the NLRP3 Inflammasome and Promote Programmed Cell Death under Irremediable ER Stress. Cell Metab, 2012. 16(2): p. 250–64. [PubMed: 22883233]
11. Upton JP, et al. IRE1alpha cleaves select microRNAs during ER stress to derepress translation of proapoptotic Caspase-2. Science, 2012. 338(6108): p. 818–22. [PubMed: 23042294]
12. Belmont PJ, et al. Regulation of microRNA expression in the heart by the ATF6 branch of the ER stress response. J Mol Cell Cardiol, 2012. 52(5): p. 1176–82. [PubMed: 22326432]
13. Walter P and Ron D, The unfolded protein response: from stress pathway to homeostatic regulation. Science, 2011. 334(6059): p. 1081–6. [PubMed: 22116877]
14. Michalak M, et al. Calreticulin, a multi-process calcium-buffering chaperone of the endoplasmic reticulum. Biochem J, 2009. 417(3): p. 651–66. [PubMed: 19133842]
15. Behrman S, Acosta-Alvear D, and Walter P, A CHOP-regulated microRNA controls rhodopsin expression. J Cell Biol, 2011. 192(6): p. 919–27. [PubMed: 21402790]
16. Afonyushkin T, Oskolkova OV, and Bochkov VN, Permissive role of miR-663 in induction of VEGF and activation of the ATF4 branch of unfolded protein response in endothelial cells by oxidized phospholipids. Atherosclerosis, 2012. 225(1): p. 50–5. [PubMed: 22776647]
17. Xu Z, et al. miR-216b regulation of c-Jun mediates GADD153/CHOP-dependent apoptosis. Nat Commun, 2016. 7: p. 11422. [PubMed: 27173017]
18. Yang J, Zhang HF, and Qin CF, MicroRNA-217 functions as a prognosis predictor and inhibits pancreatic cancer cell proliferation and invasion via targeting E2F3. Eur Rev Med Pharmacol Sci, 2017. 21(18): p. 4050–4057. [PubMed: 29028097]
19. Chen Q, et al. MicroRNA-217 inhibits cell proliferation, invasion and migration by targeting Tpd52l2 in human pancreatic adenocarcinoma. Oncol Rep, 2017. 38(6): p. 3567–3573. [PubMed: 29039566]
20. Lin Y, et al. miR-217 inhibits proliferation, migration, and invasion via targeting AKT3 in thyroid cancer. Biomed Pharmacother, 2017. 95: p. 1718–1724. [PubMed: 28962076]
21. Chen DL, et al. microRNA-217 inhibits tumor progression and metastasis by downregulating EZH2 and predicts favorable prognosis in gastric cancer. Oncotarget, 2015. 6(13): p. 10868–79. [PubMed: 25869101]
22. Guo J, et al. MicroRNA-217 functions as a tumour suppressor gene and correlates with cell resistance to cisplatin in lung cancer. Mol Cells, 2014. 37(9): p. 664–71. [PubMed: 25234467]

23. Li H, et al. MicroRNA-217, down-regulated in clear cell renal cell carcinoma and associated with lower survival, suppresses cell proliferation and migration. Neoplasma, 2013. 60(5): p. 511–5. [PubMed: 23790169]
24. He S, et al. MiR-217 Inhibits Proliferation, Migration, and Invasion by Targeting SIRT1 in Osteosarcoma. Cancer Biother Radiopharm, 2019. 34(4): p. 264–270. [PubMed: 31070483]
25. Jiang B, et al. MiR-217 Inhibits M2-Like Macrophage Polarization by Suppressing Secretion of Interleukin-6 in Ovarian Cancer. Inflammation, 2019. 42(5): p. 1517–1529. [PubMed: 31049770]
26. Zhou W, et al. miR-217 inhibits triple-negative breast cancer cell growth, migration, and invasion through targeting KLF5. PLoS One, 2017. 12(4): p. e0176395. [PubMed: 28437471]
27. Zhang M, et al. miR-217 suppresses proliferation, migration, and invasion promoting apoptosis via targeting MTDH in hepatocellular carcinoma. Oncol Rep, 2017. 37(3): p. 1772–1778. [PubMed: 28184926]
28. Wang H, et al. MiR-217 promoted the proliferation and invasion of glioblastoma by repressing YWHAG. Cytokine, 2017. 92: p. 93–102. [PubMed: 28126486]
29. Wang B, et al. MicroRNA-217 functions as a prognosis predictor and inhibits colorectal cancer cell proliferation and invasion via an AEG-1 dependent mechanism. BMC Cancer, 2015. 15: p. 437. [PubMed: 26016795]
30. Bu Y, et al. A PERK-miR-211 axis suppresses circadian regulators and protein synthesis to promote cancer cell survival. Nat Cell Biol, 2018. 20(1): p. 104–115. [PubMed: 29230015]
31. Chitnis NS, et al. miR-211 Is a Prosurvival MicroRNA that Regulates chop Expression in a PERK-Dependent Manner. Mol Cell, 2012. 48(3): p. 353–64. [PubMed: 23022383]
32. Atkins C, et al. Characterization of a novel PERK kinase inhibitor with antitumor and antiangiogenic activity. Cancer Res, 2013. 73(6): p. 1993–2002. [PubMed: 23333938]
33. Harding HP, Zhang Y, and Ron D, Protein translation and folding are coupled by an endoplasmic-reticulum-resident kinase. Nature, 1999. 397(6716): p. 271–4. [PubMed: 9930704]
34. Shi Y, et al. Identification and characterization of pancreatic eukaryotic initiation factor 2 alpha-subunit kinase, PEK, involved in translational control. Mol Cell Biol, 1998. 18(12): p. 7499–509. [PubMed: 9819435]
35. Harding HP, et al. Regulated translation initiation controls stress-induced gene expression in mammalian cells. Mol Cell, 2000. 6(5): p. 1099–108. [PubMed: 11106749]
36. Vattem KM and Wek RC, Reinitiation involving upstream ORFs regulates ATF4 mRNA translation in mammalian cells. Proc Natl Acad Sci U S A, 2004. 101(31): p. 11269–74. [PubMed: 15277680]
37. Harding HP, et al. An integrated stress response regulates amino acid metabolism and resistance to oxidative stress. Mol Cell, 2003. 11(3): p. 619–33. [PubMed: 12667446]
38. Ma Y, et al. Two distinct stress signaling pathways converge upon the CHOP promoter during the mammalian unfolded protein response. J Mol Biol, 2002. 318(5): p. 1351–65. [PubMed: 12083523]
39. Gonzalez S, Pisano DG, and Serrano M, Mechanistic principles of chromatin remodeling guided by siRNAs and miRNAs. Cell Cycle, 2008. 7(16): p. 2601–8. [PubMed: 18719372]
40. Li JH, et al. starBase v2.0: decoding miRNA-ceRNA, miRNA-ncRNA and protein-RNA interaction networks from large-scale CLIP-Seq data. Nucleic Acids Res, 2014. 42(Database issue): p. D92–7. [PubMed: 24297251]
41. Laugesen A and Helin K, Chromatin repressive complexes in stem cells, development, and cancer. Cell Stem Cell, 2014. 14(6): p. 735–51. [PubMed: 24905164]
42. Varambally S, et al. The polycomb group protein EZH2 is involved in progression of prostate cancer. Nature, 2002. 419(6907): p. 624–9. [PubMed: 12374981]
43. Okosun J, et al. Integrated genomic analysis identifies recurrent mutations and evolution patterns driving the initiation and progression of follicular lymphoma. Nat Genet, 2014. 46(2): p. 176–181. [PubMed: 24362818]
44. Sneeringer CJ, et al. Coordinated activities of wild-type plus mutant EZH2 drive tumor-associated hypertrimethylation of lysine 27 on histone H3 (H3K27) in human B-cell lymphomas. Proc Natl Acad Sci U S A, 2010. 107(49): p. 20980–5. [PubMed: 21078963]

45. Ernst T, et al. Inactivating mutations of the histone methyltransferase gene EZH2 in myeloid disorders. Nat Genet, 2010. 42(8): p. 722–6. [PubMed: 20601953]
46. Norfo R, et al. miRNA-mRNA integrative analysis in primary myelofibrosis CD34+ cells: role of miR-155/JARID2 axis in abnormal megakaryopoiesis. Blood, 2014. 124(13): p. e21–32. [PubMed: 25097177]
47. Guglielmelli P, et al. The number of prognostically detrimental mutations and prognosis in primary myelofibrosis: an international study of 797 patients. Leukemia, 2014. 28(9): p. 1804–10. [PubMed: 24549259]
48. Nikoloski G, et al. Somatic mutations of the histone methyltransferase gene EZH2 in myelodysplastic syndromes. Nat Genet, 2010. 42(8): p. 665–7. [PubMed: 20601954]
49. Ntziachristos P, et al. Genetic inactivation of the polycomb repressive complex 2 in T cell acute lymphoblastic leukemia. Nat Med, 2012. 18(2): p. 298–301. [PubMed: 22237151]
50. Zhang J, et al. The genetic basis of early T-cell precursor acute lymphoblastic leukaemia. Nature, 2012. 481(7380): p. 157–63. [PubMed: 22237106]

Implications:

PERK-dependent induction of miR-217 limits accumulation and function of the pro-survival micro-RNA, miR-211, to establish cell fate and promote cell commitment to apoptosis.

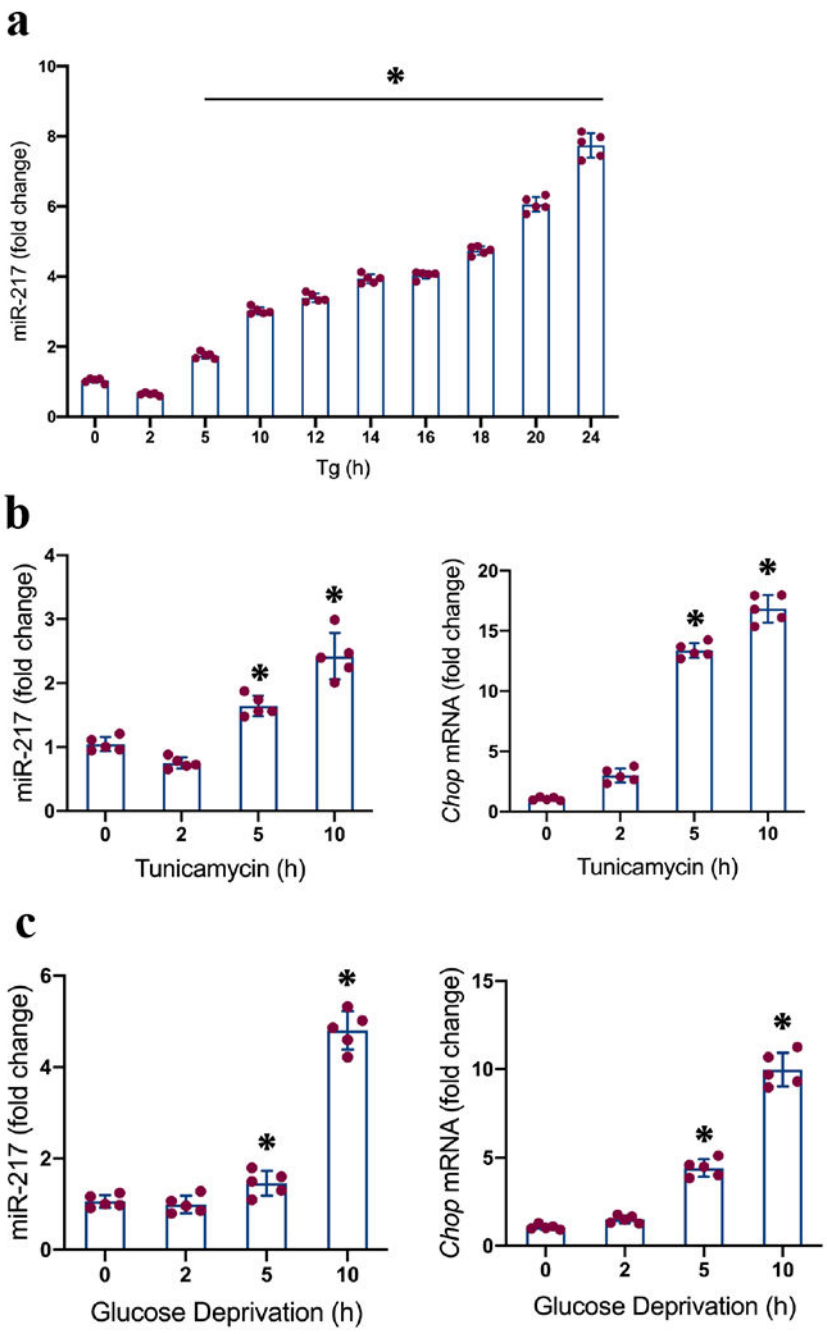

Figure 1: ER stress induced miR-217 expression.

(a,b) qPCR analysis of miR-217 expression and *Chop* mRNA levels in NIH3T3 cells treated with thapsigargin (Tg, 300nM) or Tunicamycin (1mg/ml) for indicated times. Averages are calculated from five independent experiments. (c) qPCR analysis of miR-217 expression and *Chop* mRNA levels in NIH3T3 cells cultured in low-glucose medium for indicated times. Data are mean ± s.d. of five independent experiments. Statistical analysis was analyzed by Student's t-test. (*P<0.05, treatment versus non-treatment).

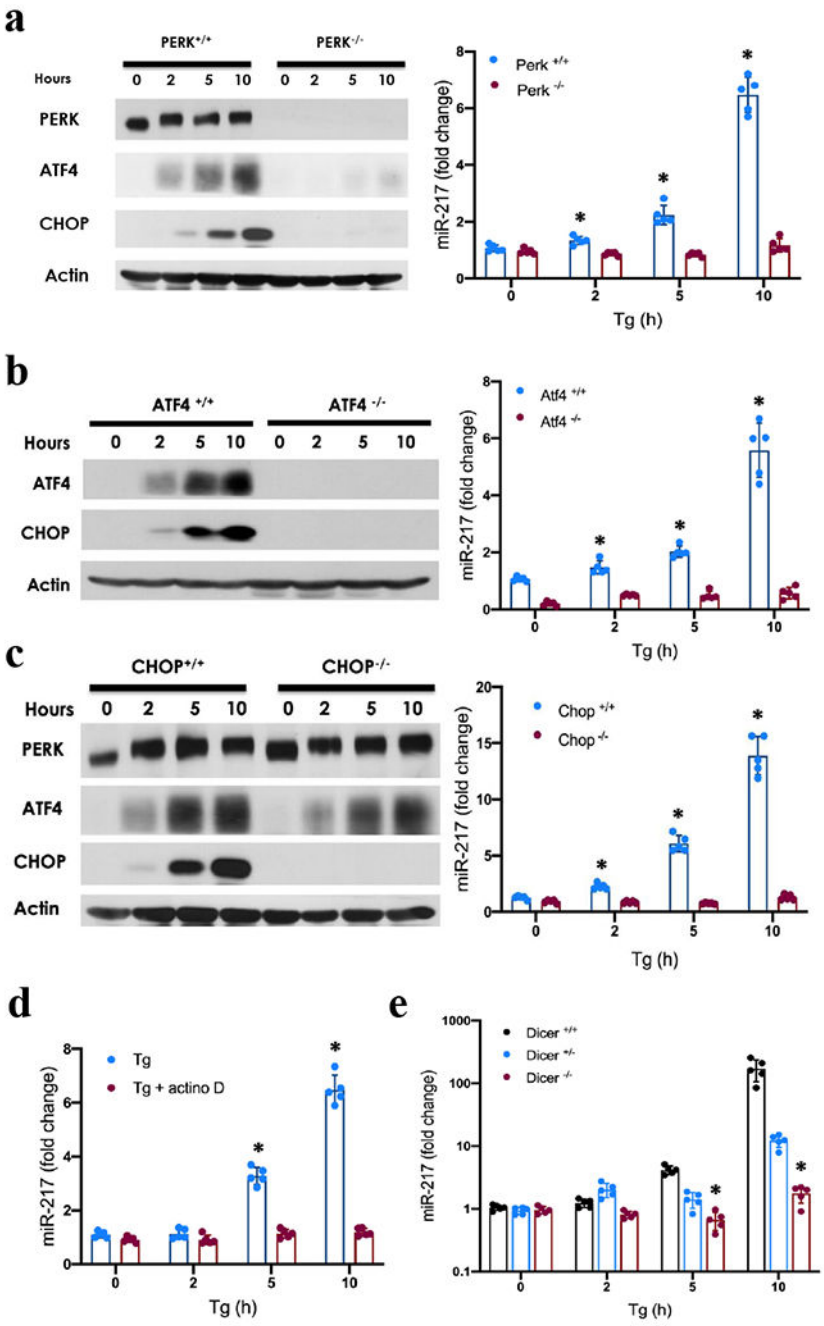

Figure 2: miR-217 induction is PERK, ATF4 and CHOP-dependent.

(a) PERK$^{+/+}$ and PERK$^{-/-}$ MEFs were treated with Tg (300nM) for indicated times. PERK, ATF4, and CHOP expression was assessed by immunoblot (left) and miR-217 expression by qPCR (right graph). (b, c) MEFs of the indicated genotype were treated with Tg (300nM) for indicated intervals. Lysates were immunoblotted for the proteins indicated (left panels) and miR-217 levels quantified by qPCR (right panels; n=3). (d) NIH3T3 cells were treated with/without actinomycin D (2mg/ml) for 1h and challenged with 300nM Tg as indicated. MiR-217 levels were quantified by qPCR (mean ± s.d., n=3). (e) Dicer$^{+/+}$, Dicer$^{+/-}$ and

Dicer$^{-/-}$ MEFs were treated with Tg (300nM) as indicated, followed by qPCR assessment of miR-217. Data represent mean ± s.d. of five independent experiments and statistical analysis was analyzed by Student's t-test (*P < 0.05).

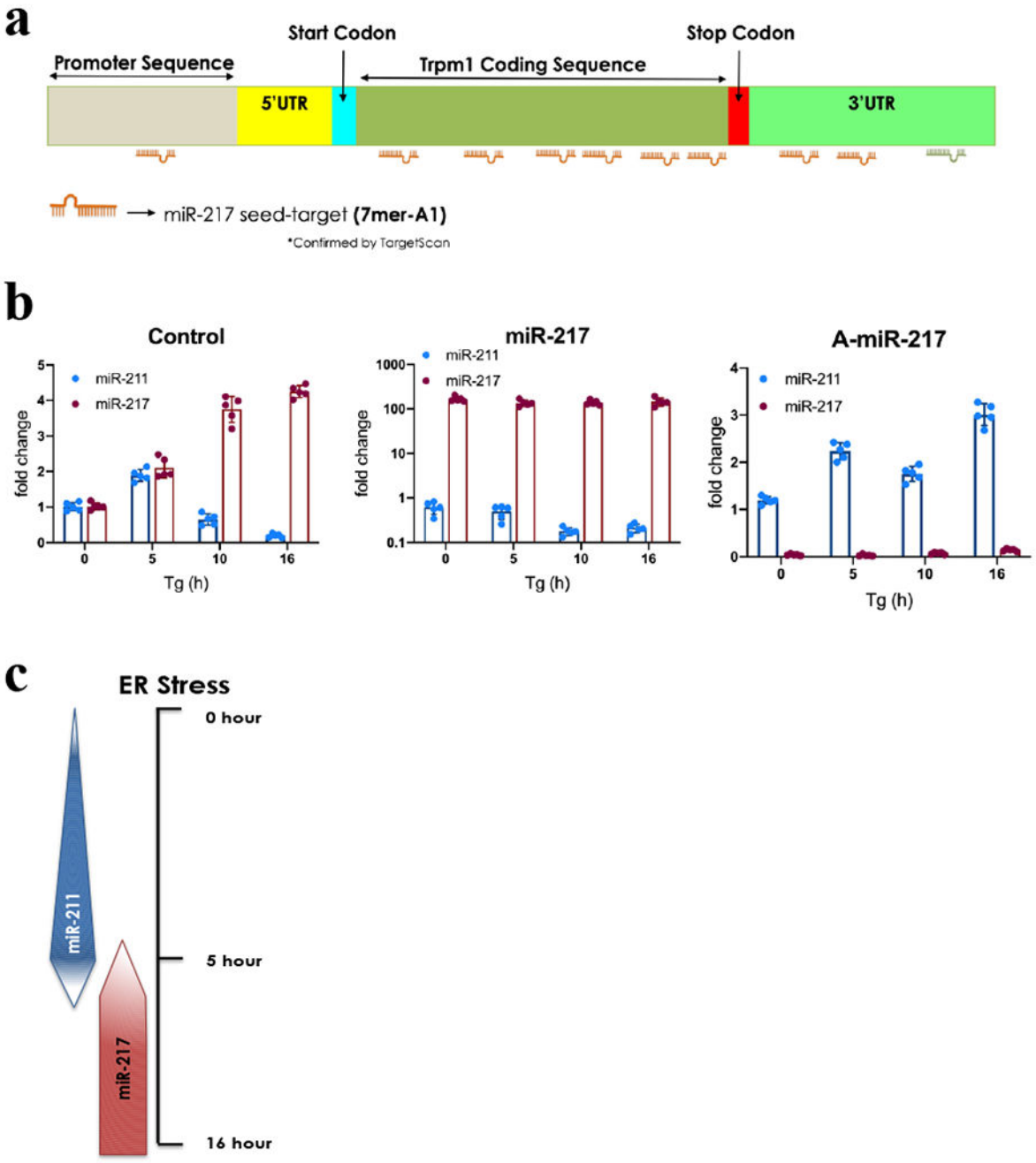

Figure 3. Regulatory tension of miR-211 and miR-217 under ER-stress.

(a) Schematic representation of *Homo sapiens* transient receptor potential cation channel subfamily M member 1 (*Trpm1*), mRNA. (b) AGS cells expressing control, miR-217, or A-miR-217 were treated as indicated and RNA was isolated for qPCR to quantify the expression levels of miR-211 (blue) and miR-217 (red). Data represent mean ± s.d. of five independent experiments.

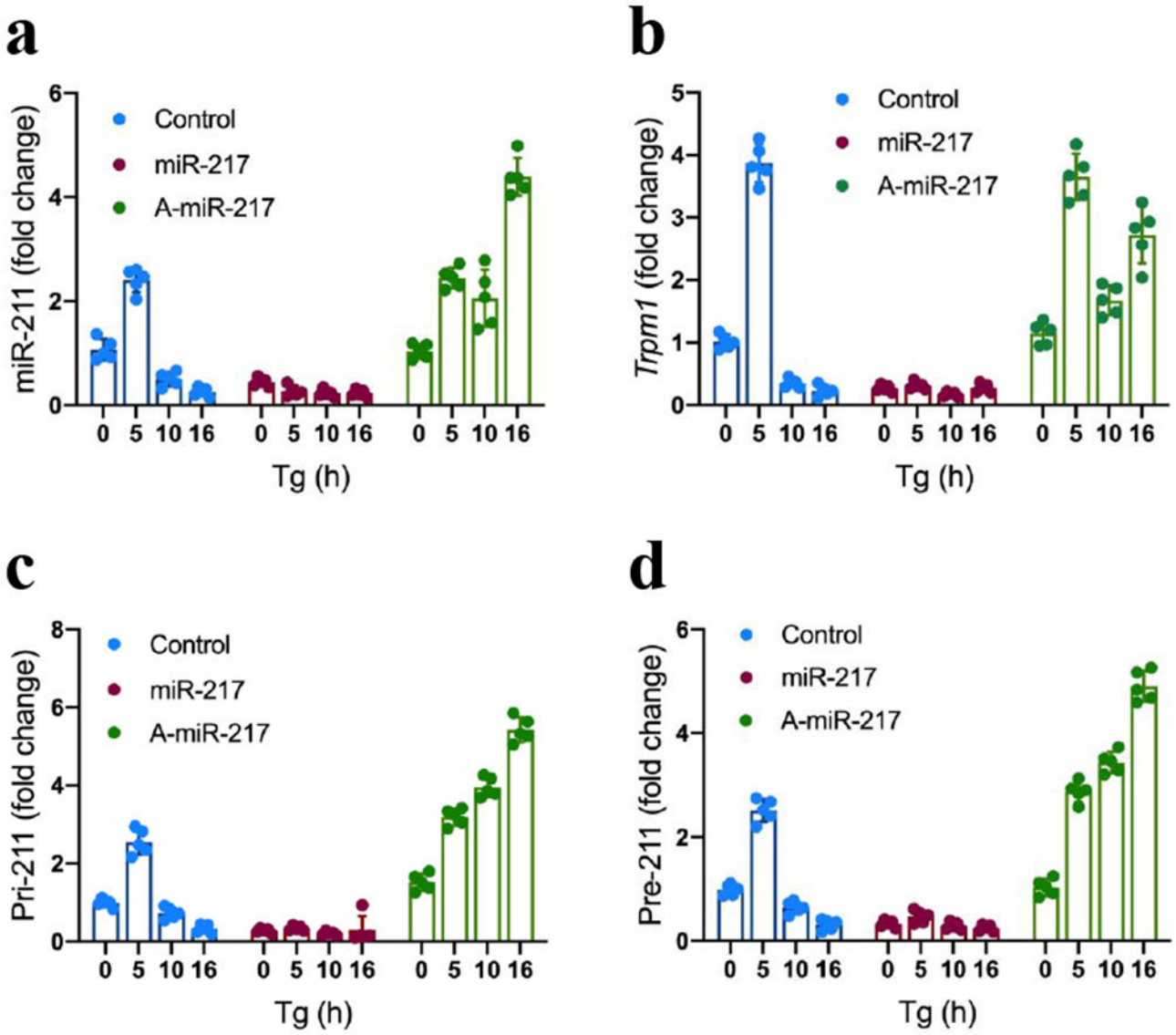

Figure 4: miR-217 regulates the expression of Pri-211, pre-211 and mature miR-211.

AGS cells expressing control, miR-217, or A-miR-217 were treated with Tg (300nM) as indicated. RNA was isolated from the treated cells and qPCR was used to quantify the following: (a) Expression level of mature miR-211; (b) Expression level of *Trpm1:* (c) Expression level of Pri-miR-211; (d) Expression level of Pre-miR-211. Data represent mean ± s.d. of five independent experiments. (e) Schematic representation of acute ER stress induced regulation of miR-211 by miR-217.

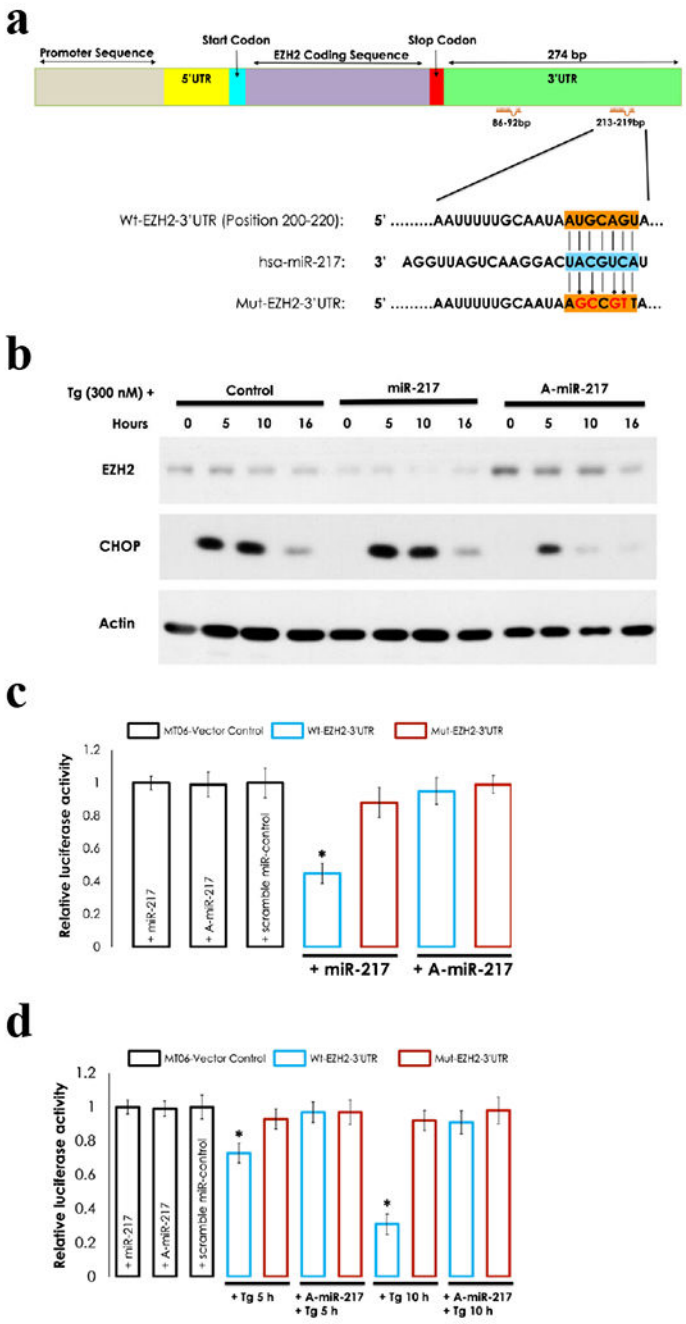

Figure 5: EZH2 is a direct target of miR-217.

(a) Schematic representation of sequence alignment of miR-217 with different species of the EZH2 3'-UTR. The seed sequence of miR-217 (Blue) matches the two seed recognizing sites of the EZH2 3'UTR (Orange). From the wildtype (Wt), a single seed recognizing site mutated EZH2-3'UTR (Mut-EZH2-3'UTR, with the substituted bases marked in Red), was generated. (b) Ectopic miR-217 expression reduces EZH2 protein levels in contrast to A-miR-217. (c) ER stress regulates EZH2 expression via miR-217 induction: 3'UTR-Vector Control or Wt-EZH2-3'UTR or Mut-EZH2-3'UTR reporter construct was independently

expressed in scrambled control, miR-217, and A-miR-217 expressing NIH3T3 cells, respectively. (d) Cells were exposed to Tg (300nM) for 5 or 10 hrs. (e) Firefly luciferase (*hLuc*) activity was measured and normalized to transfection control Synthetic Renilla Luciferase. Error bars represent standard deviation for three independent experiments. Data represent mean ± s.d. of three independent experiments and statistical analysis was analyzed by Student's t-test (*P < 0.05).

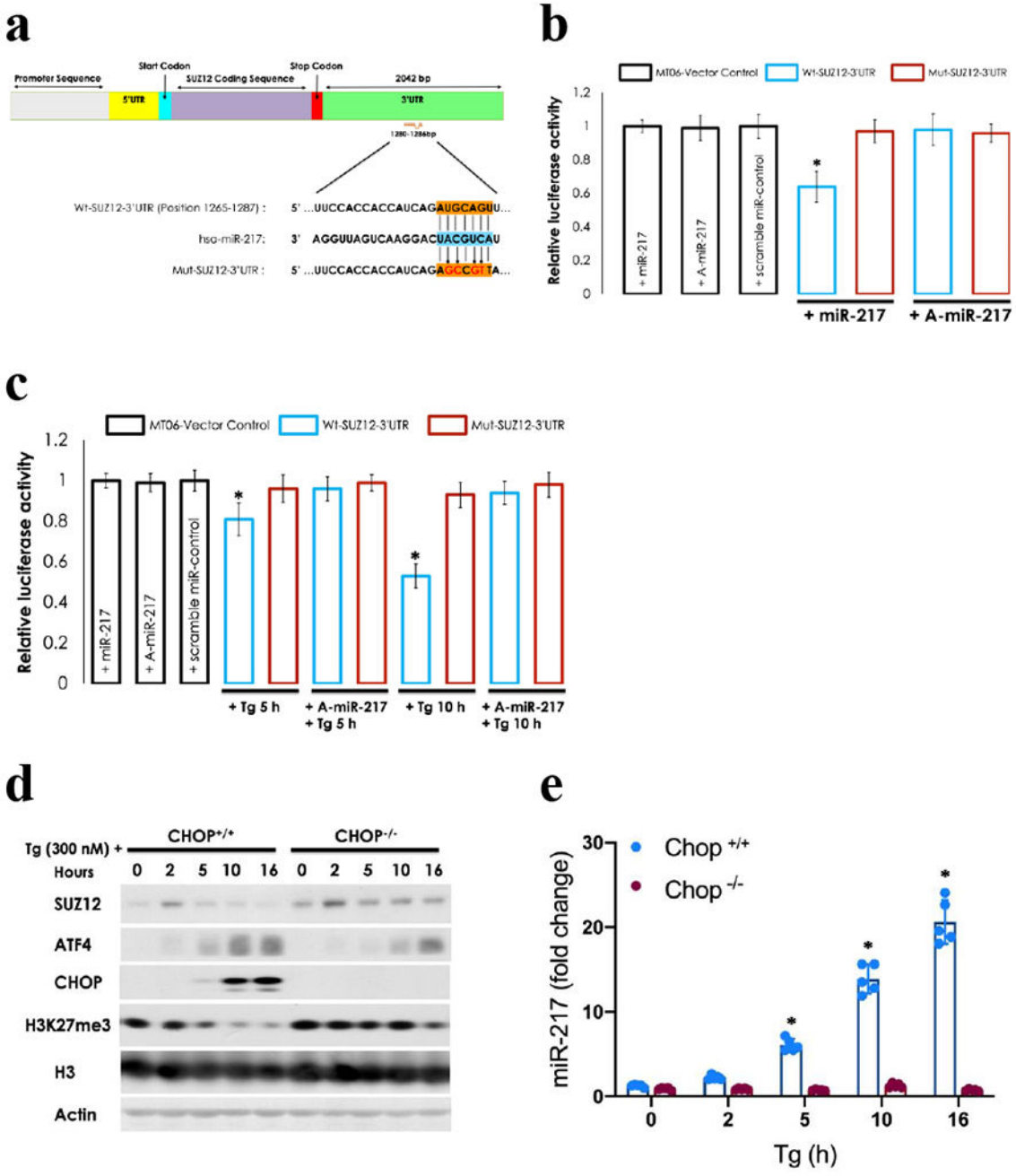

Figure 6: SUZ12 is a direct target of miR-217.

(a) Schematic representation of sequence alignment of miR-217 with different species of the SUZ12 3'-UTR. The seed sequence of miR-217 (Blue) matches in the seed recognizing site of the SUZ12 3'UTR (Orange). From the wildtype (Wt-SUZ12-3'UTR), the seed mutations were generated in SUZ12-3'UTR (Mut-SUZ12-3'UTR, with the substituted bases marked in Red). (b) 3'UTR-Vector Control or Wt-SUZ12-3'UTR or Mut-SUZ12-3'UTR reporter construct was independently expressed in scrambled miR-control, miR-217 and A-miR-217 expressing NIH3T3 cells, respectively. (c) Cells were exposed to Tg (300nM) for either 5

or 10 hrs and firefly luciferase (*hLuc*) activity was measured and normalized to Renilla Luciferase. Error bars represent standard deviation for three independent experiments. (d) miR-217 mediated inactivation of SUZ12 results in global decrease in cellular H3K27me3 level. $CHOP^{+/+}$ and $CHOP^{-/-}$ MEFs were treated with Tg (300nM) for indicated times. ATF4, CHOP, H3K27me3, H3 and actin were assessed by immunoblot. (e) miR-217 levels were assessed by qPCR following Tg (300nM) exposure to $CHOP^{+/+}$ and $CHOP^{-/-}$ MEFs for the indicated time-points. Data represent mean ± s.d. of five independent experiments and statistical analysis was analyzed by Student's t-test (*$P < 0.05$).

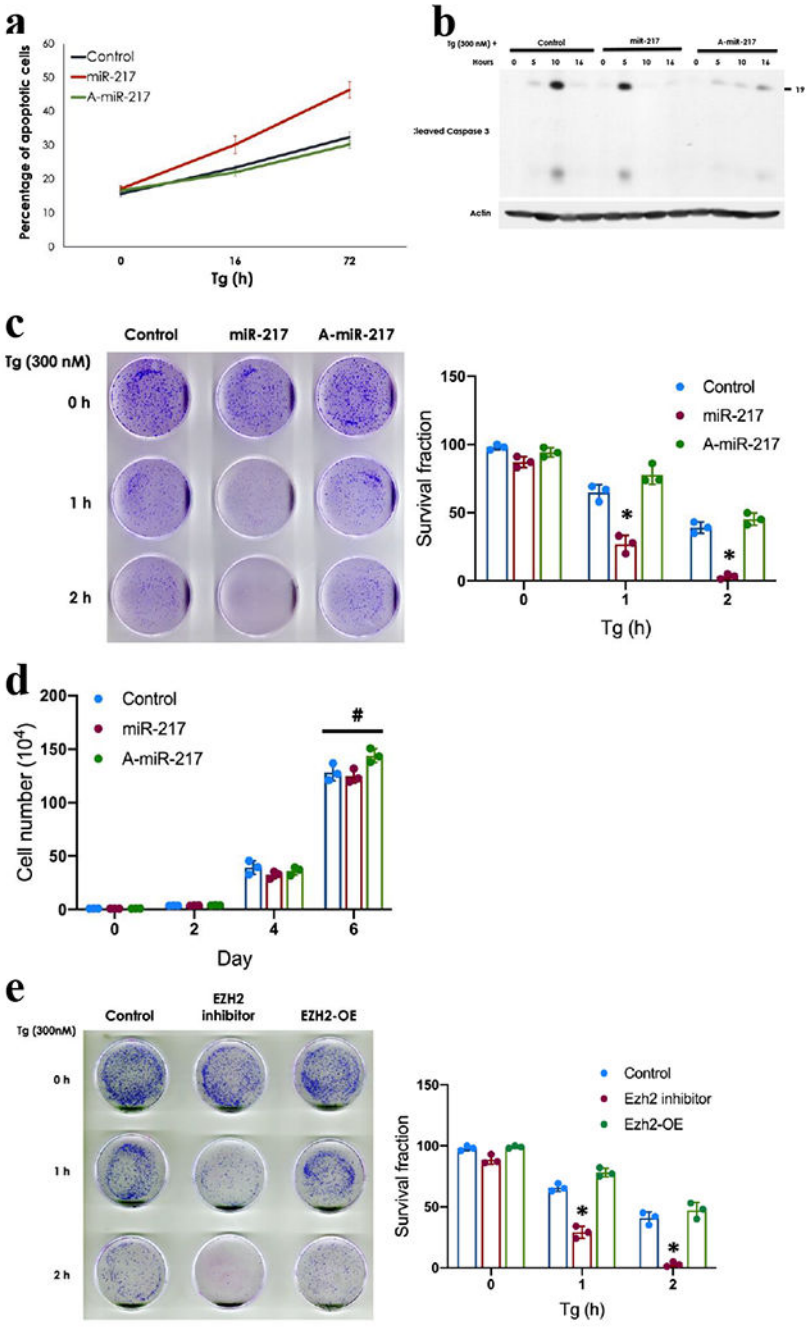

Figure 7: miR-217 expression sensitizes cells to ER stress.

(a) Annexin V was quantified by FACS of AGS cells expressing control, miR-217, or A-miR-217 following treatment with Tg (300nM) for indicated intervals. (b) Cleaved Caspase 3 was quantified by immunoblot from cells treated as indicated. (c) Clonogenic survival of AGS cells stably expressing control, miR-217 or A-miR-217 were treated with Tg (300nM) for 0, 1 or 2 hr. Quantification of colonies (right). (d) Cell doubling was quantified over 6 days. Values are means ± s.d. (n=3) and statistical significance was analyzed by Student's t-test. (*P<0.05; #P>0.05). (e) Clonogenic survival of AGS cells stably expressing control, or

EZH2 (EZH2-OE) and treated with Tg (300 nM) for 0, 1 or 2 hr in presence or in absence of EZH2 inhibitor. Quantification of colonies (right).